Highly polarized emission of the liquid crystalline conjugated polymer by controlling the surface anchoring energy

2014 Jpn. J. Appl. Phys. 53 03CD04

(http://iopscience.iop.org/1347-4065/53/3S1/03CD04)

Japanese Journal of Applied Physics **53**, 03CD04 (2014) **REGULAR PAPER**
http://dx.doi.org/10.7567/JJAP.53.03CD04

Highly polarized emission of the liquid crystalline conjugated polymer by controlling the surface anchoring energy

Soo In Jo[1], Youngsik Kim[2], Ji-Ho Baek[2], Chang-Jae Yu[1,2], and Jae-Hoon Kim[1,2*]

[1]*Department of Electronic Engineering, Hanyang University, Seoul 133-791, Korea*
[2]*Department of Information Display Engineering, Hanyang University, Seoul 133-791, Korea*
E-mail: jhoon@hanyang.ac.kr

Received July 9, 2013; accepted October 27, 2013; published online February 17, 2014

We demonstrated a highly polarized organic light-emitting diode (OLED) through the enhancement of the orientational ordering of the emitting polymer with a nematic liquid crystalline (LC) phase. The highly ordered state of the conjugate polymer was obtained by thermal annealing at the nematic temperature and strong azimuthal anchoring energy of the underlying polyimide. The order parameter of the conjugate polymer was analyzed using a second-harmonic generation model and the dichroic ratio was measured to be 22 : 1. Also, we applied our optimized OLED with high optical polarizability to an effective light source for a twisted nematic LC display.

1. Introduction

Organic electroluminescence (EL) phenomena have been studied for a display application of an organic light-emitting diode (OLED), owing to their excellent characteristics such as low voltage driving, high brightness, and good color performance.[1)] In particular, polymer light-emitting diodes (PLEDs) based on a solution process have attracted considerable attention because of their low-cost fabrication process.[2)] In PLEDs, the emitted light is strongly affected by the orientation of the conjugated polymer. The polarization state of the emitting light is governed by the azimuthal ordering of the conjugated polymer and manipulated by its azimuthal direction. To obtain a polarized light from OLEDs, various approaches, such as stretching, Langmuir–Blodgett (LB) deposition, the use of nanostructures, and direct rubbing, were proposed.[3–19)] However, those approaches are unsuitable for large-size applications.[20)] Additionally, a photon recycling method with an external compensation layer was applied to realize a high polarization ratio (50 : 1), but it is difficult to adopt it in large-scale manufacturing owing to the complex fabrication process of giant birefringent optics films.[21)]

Liquid crystalline (LC) fluorescent materials can easily be aligned by a simple rubbing process to an alignment layer, such as a large polyimide (PI) or hole transport layer.[22)] As a result, a high optical polarizability is expected to be obtained owing to the LC feature of the emitting polymer.

In general, the rubbing process governs the distribution of the polymer backbone in an alignment layer. Thus, the polymer backbone distribution is directly transferred to the LC fluorescent orientation. In this situation, the interfacial interaction between the alignment layer and the LC fluorescent material is strongly converted to the azimuthal anchoring energy. The anchoring energy is generally affected by rubbing conditions including surface defects, such as scratches. Jandke et al. reported the disadvantages of surface scratches in polarized OLEDs and introduced the use of an additional emission layer to obtain a highly polarized emission.[5)] For polarized OLEDs, the relationship between anchoring energy and optical polarizability is quantitatively investigated to obtain high performances. However, such a relationship has not been fully investigated yet.

In this study, we investigated the optical polarizability of an OLED that corresponds to the surface anchoring energy produced by an underlying rubbed polymer. The orientational order parameter of the conjugated polymer was analyzed from polarization-dependent photoluminescence (PL) using a second-harmonic generation (SHG) model.[23)] Using this method, we obtained optimized conditions for the alignment layer for highly polarized OLEDs. Also, we demonstrated a twisted nematic (TN) LCD with high light efficiency using a highly polarized OLED as an effective light source.

2. Experimental procedure

Poly(9,9-di-*n*-octylfluorenyl-2,7-diyl)-*alt*-(benzo[2,1,3]thiadiazol-4,8-diyl)] (F8BT from American Dye Source) with a nematic LC phase was used as an emitting layer for the highly polarized OLED. To improve the azimuthal ordering of the emitting polymer, an AL22620 PI layer (from JSR) was spin-coated onto an indium–tin oxide (ITO) substrate, as shown in Fig. 1. The thickness of the PI layer was selected to be about 10 nm to minimize the insulating effect of the PI layer. After thermal imidization on a hot plate, the PI layer was rubbed using a cotton roller at different times to control the azimuthal anchoring energy of the alignment surface for the emitting polymer. The polymer film was unidirectionally rubbed by a rubbing machine with a 6.5-cm-diameter roller covered with a cotton cloth. The roller speed and the speed of the substrate stage were fixed at 500 rpm and 6 mm/s, respectively.

The F8BT layer dissolved in toluene was spin-coated onto the rubbed PI layer. The thickness of the F8BT layer was measured to be about 60 nm. Initially, the emitting polymers were randomly oriented in azimuthal directions as shown in Fig. 1(d), owing to the randomness of the spin-coating process. To increase the azimuthal ordering of the F8BT layer, the prepared substrate was annealed at the nematic temperature of the F8BT layer onto the hot plate for 20 min. The unidirectional alignment of the emitting polymer is clearly shown in the inset textures of Fig. 1(e) under crossed polarizers. Note that the bright texture was obtained under crossed polarizers when the alignment direction of the nematic LC was rotated by 45° with respect to one of the crossed polarizers. Finally, Ca/Al layers with thicknesses of 5 and 9 nm were deposited by thermal evaporation,

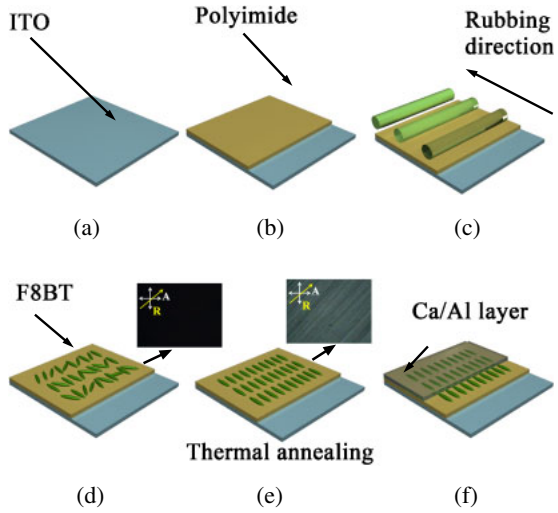

Fig. 1. (Color online) Schematic diagrams of the fabrication of polarized OLED: (a) ITO layer as anode, (b) PI layer as alignment layer, (c) rubbing process, (d) spin coating of the F8BT layer, (e) thermal annealing process, and (f) Ca/Al deposition as cathode.

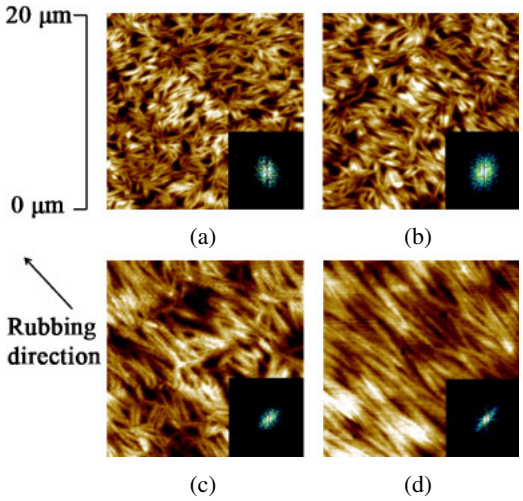

Fig. 3. (Color online) Measured AFM images of the F8BT layers with (a) 1, (b) 3, (c) 5, and (d) 7 rubbings after thermal annealing. The insets exhibit 2D FFT images. An arrow depicts the rubbing direction.

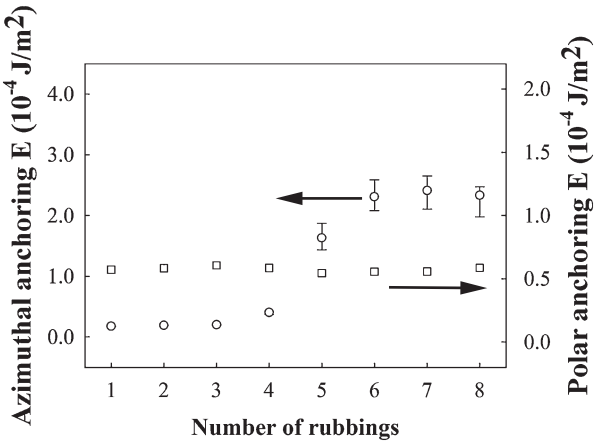

Fig. 2. Measured anchoring energy of the alignment layer. Circles and squares represent the azimuthal and polar anchoring energies, respectively.

respectively [Fig. 1(f)]. All processes were carried out in a glove box filled with Ar gas to avoid exposure to humidity and oxygen. We also fabricated a conventional TN LC sample by applying a highly polarized OLED as a backlight unit. For fabricating a TN cell, two ITO substrates with a rubbed PI layer were assembled perpendicular and the cell gap was maintained about 4.7 μm with glass spacers. An LC with positive dielectric anisotropy ($\Delta\varepsilon = 5.5$) was injected in an isotropic phase using capillary force.

3. Results and discussion

We measured the surface anchoring energy of the PI layer according to the rubbing condition to quantify the surface characteristics. The anchoring energy of the alignment layer is generally represented by the Rapini–Papoular anchoring potential form.[24] Figure 2 shows the measured anchoring energy characteristics of the PI layer as a function of the number of rubbings. The azimuthal and polar anchoring energies were estimated by a torque balance method and a high field method, respectively.[25,26] In the non rubbed PI layer, the PI polymers promote a planar alignment, but they are randomly oriented without any preference in the azimuthal direction; thus, the PI film is isotropic. After rubbing, however, the azimuthal symmetry is broken and the directional preference generates the azimuthal anchoring energy. With increasing ordering of the PI layer by rubbing, the azimuthal anchoring energy rapidly increases and finally saturates after 7 rubbings owing to the limitation of the polymer chain ordering.[27] In fact, the scratch produced by rubbing was clearly observed in the substrate rubbed 8 times. On the other hand, the polar anchoring energy is almost constant irrespective of the number of rubbings, since it is not strongly affected by the azimuthal ordering of the polymer but by molecular interaction.[28]

Initially, the spin-coated F8BT layer shows an isotropic distribution even on the anisotropic PI layer. During the thermal annealing process, the nematic phase transition occurs in the F8BT layer; thus, the F8BT layer is unidirectionally aligned according to the rubbing direction. The azimuthal ordering of the F8BT domains on the rubbed PI layer was investigated by surface morphology analysis with atomic force microscope (AFM; Park Systems XE-100). As shown in Fig. 3, with increasing number of rubbings and resultant azimuthal anchoring energy, the anisotropy of the surface morphology is clearly observed. The direction of the anisotropy directly corresponds to the rubbing direction. The two-dimensional (2D) fast Fourier transformation (FFT) clearly reflects the anisotropy of the surface morphology, as shown in Fig. 3 (see inset figures in the AFM images). The direction of the 2D FFT result reveals the power spectra of the periodic morphology in the perpendicular direction. In Fig. 3(a), the 2D FFT is circular owing to the random periodicities of the molecules. However, by increasing the number of rubbings, the periodicities of the molecules are arranged in predefined directions and the 2D FFT becomes an anisotropic ellipse. Also, from the AFM textures and the corresponding 2D FFT images, the anisotropy of the F8BT layer is definitely observed from a sample rubbed 5 times and the above one similar to the results of the azimuthal

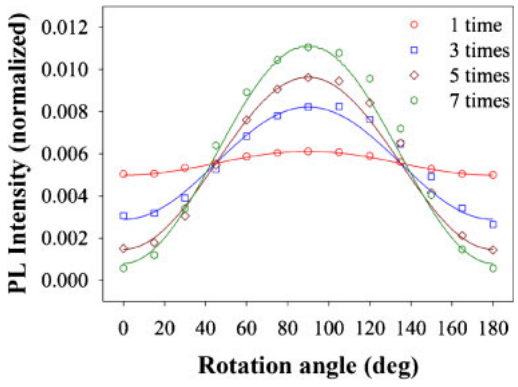

(a)

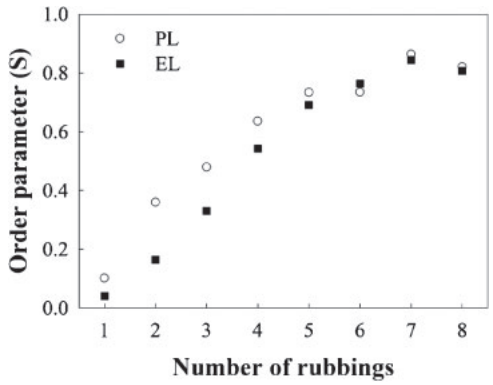

(b)

Fig. 4. (Color online) (a) PL intensities of the fabricated samples as a function of the polarization angle and (b) the order parameters evaluated using the SHG model.

anchoring energy, that is, the azimuthal anchoring energy significantly increases after 5 rubbings. As a result, the azimuthal anchoring energy of the underlying surface strongly affects the molecular ordering of the F8BT layer.

The optical polarizability of the F8BT layer depending on the azimuthal anchoring energy was investigated through the PL measurements shown in Fig. 4. The polarization-dependent PL intensity was measured by rotating a polarizer in front of a detector. In general, the polarization of light emitted from the conjugated polymer coincides with the direction of the conjugated backbone. Therefore, each polarization component generated by polarized excitation reflects the molecular distribution of the conjugated backbone.[29] Figure 4 shows the measured PL characteristics of the differently rubbed samples as a function of the rotation angle of the polarizer. Here, the rubbing direction is selected to be 90°. To estimate the order parameter of the backbone orientation, we adopt the SHG model under a constraint of in-plane ordering. Note that the PL intensity is proportional to the absorption, and thus the polarization dependence of the PL intensity is directly related to that of the backbone orientation. The measured intensity by varying the polarizer angle (ϕ) was fitted using the following equation in the SHG model:[23]

$$g(\theta,\phi) = F\exp\left(-\frac{\theta-\pi/2}{2\sigma^2}\right)\left(1+\sum_{\infty}^{n=1} a_n \cos n\phi\right),$$

where θ and σ are the polar angle of the substrate and the standard deviation of the polar angle, respectively. The first

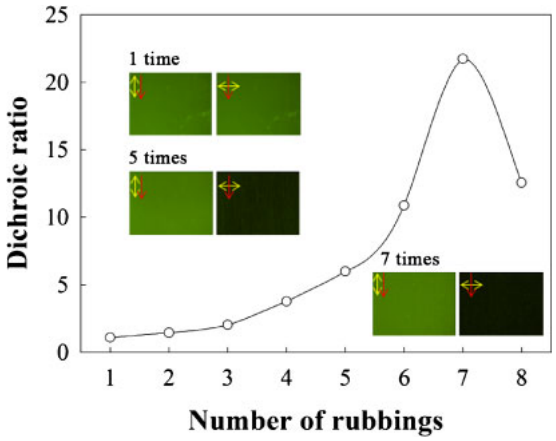

Fig. 5. (Color online) Measured dichroic ratios of the fabricated EL samples and microscopic textures with one polarizer.

Gaussian distribution term is negligible in the in-plane model, since we assume that most polymer backbones lie on the substrate plane.

Now, we calculate the in-plane order parameter from the fitting parameter that corresponds to the amplitude of n-th-order harmonics and an orientational order parameter. At the polarization-dependent PL intensity, with increasing number of rubbings (the azimuthal anchoring energy), the optical polarizability and resultant order parameter increased, as shown in Fig. 4. As aforementioned, since the rubbing scratch was clearly observed in the substrate rubbed 8 times, the order parameter degraded after right rubbings. In fact, since the thin PI layer was used for minimizing the insulating effect of the additive alignment layer, the PI layer was easily damaged by a strong rubbing. The maximum value of the order parameter (~0.9) is also comparable to that observed in conventional rubbed nematic LC cases.[30] We also obtain results similar to the order parameters estimated from the polarization-dependent EL intensity, as shown in Fig. 4(b).

Figure 5 shows the dichroic ratios of the OLEDs fabricated under different rubbing conditions. As expected, the dichroic ratio rapidly increases up to 7 rubbings and then decreases at the 8th rubbing. The inset images show the EL images of the OLED samples under different polarizer angles prepared by 1, 5, and 7 rubbings. When the rubbing direction is parallel to the transmission axis of the polarizer, the maximum brightness is obtained. Figure 6 shows the current–voltage and luminescence–voltage characteristics of an OLED cell rubbed 7 times. In the OLED rubbed 7 times, the luminescence was measured to be about 1200 cd/m^2 at 12 V and the dichroic ratio was about 22 : 1.

On the basis of the high optical polarizability of our proposed OLED, we also demonstrated a TN LCD with high light efficiency. As expected, half of the incident intensity of a nonpolarized backlight unit is blocked by the polarizer, sufficiently degrading the light efficiency in the LCDs. The highly polarized OLED was used as the backlight unit for the TN LCD. Figure 7 shows the voltage–transmittance characteristics of two TN LC cells adopted in the polarized and normal OLEDs under the same fabrication conditions. Inset images show the corresponding TN LC cells. Under crossed polarizers, the polarized OLED-adopted TN LC cell is twice

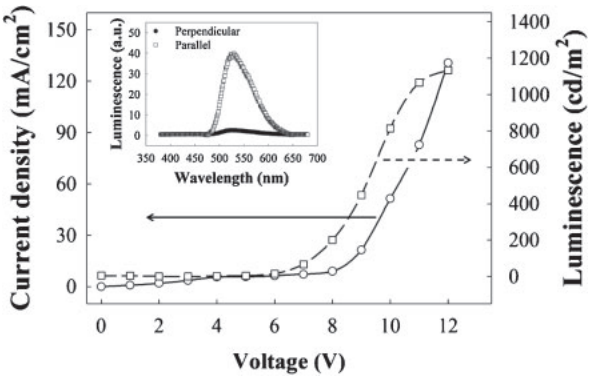

Fig. 6. Current–voltage and luminescence–voltage characteristics of OLED cell rubbed 7 times. The inset graph indicates the EL spectrum of the sample.

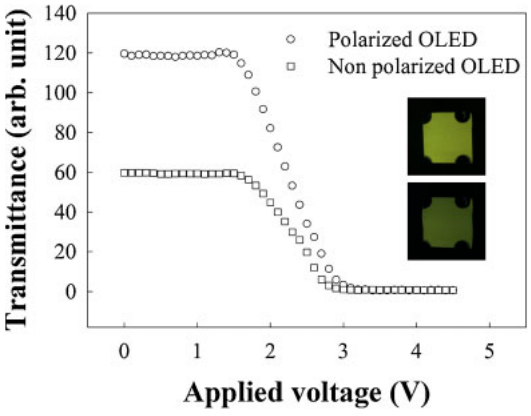

Fig. 7. (Color online) Measured voltage–transmittance characteristics of the TN LC cells with the polarized and normal OLEDs, and the corresponding camera textures of TN LC cells.

brighter than the normal one as shown in Fig. 7. Here, the polarizer is parallel to the polarization direction of the OLED.

4. Conclusions

We investigated a highly polarized OLED through the enhancement of the azimuthal ordering of the conjugate polymer with an LC phase. The highly ordered state of the emitting polymer was achieved by thermal annealing at the nematic temperature and strong azimuthal anchoring energy of the underlying PI. The order parameter of the conjugate polymer was analyzed using a SHG model and the maximum dichroic ratio of the OLED was estimated to be 22 : 1. We expect that this value will be improved by photorecycling. Also, we demonstrated a highly efficient TN LCD using our optimized OLED with high optical polarizability as an effective light source. In a commercial OLED, since the polarized sheet in front of the OLED panel is laminated for image visibility in an ambient light environment, the light efficiency is reduced by the polarizer similarly to that in the LCDs. The polarized OLED would eliminate such a reduction in light efficiency in conventional OLEDs. We believe that the polarized OLED is a viable candidate for displays with high light efficiency.

Acknowledgment

This research was supported by the IT R&D program of MKE/KEIT (Grant No. 10041416, The core technology development of light and space adaptable new mode display for energy saving on 7 inch and 2 W) and LG Display Co., Ltd.

1) K. T. Kamtekar, A. P. Monkman, and M. R. Bryce, Adv. Mater. **22**, 572 (2010).
2) J. H. Burroughes, D. D. C. Bradley, A. R. Brown, R. N. Marks, K. Mackay, R. H. Friend, P. L. Burns, and A. B. Holmes, Nature **347**, 539 (1990).
3) M. Grell and D. D. C. Bradley, Adv. Mater. **11**, 895 (1999).
4) P. Dyreklev, M. Berggren, O. Inganäs, M. R. Andersson, O. Wennerström, and T. Hjertberg, Adv. Mater. **7**, 43 (1995).
5) M. Jandke, P. Strohriegl, J. Gmeiner, W. Brutting, and M. Schwoerer, Synth. Met. **11**, 18 (1999).
6) V. Cimrová, M. Remmers, D. Neher, and G. Wegner, Adv. Mater. **8**, 146 (1996).
7) M. Grell, W. Knoll, D. Lupo, A. Meisel, T. Miteva, D. Neher, H.-G. Nothofer, U. Scherf, and A. Yasuda, Adv. Mater. **11**, 671 (1999).
8) D. Neher, Adv. Mater. **7**, 691 (1995).
9) M. Misaki, Y. Ueda, S. Nagamatsu, M. Chikamatsu, Y. Yoshida, N. Tanigaki, and K. Yase, Appl. Phys. Lett. **87**, 243503 (2005).
10) M. Misaki, Y. Ueda, S. Nagamatsu, Y. Yoshida, N. Tanigaki, and K. Yase, Macromolecules **37**, 6926 (2004).
11) A. Bolognesi, G. Bajo, J. Paloheimo, T. Östergärd, and H. Stubb, Adv. Mater. **9**, 121 (1997).
12) S. Schwiegk, T. Vahlenkamp, G. Wegner, and Y. Xu, Thin Solid Films **210–211**, 6 (1992).
13) S. Schwiegk, T. Vahlenkamp, Y. Xu, and G. Wegner, Macromolecules **25**, 2513 (1992).
14) K. Sakamoto, K. Usami, Y. Uehara, and S. Ushioda, Appl. Phys. Lett. **87**, 211910 (2005).
15) Z. Hu, G. Baralia, V. Bayot, J.-F. Gohy, and A. M. Jonas, Nano Lett. **5**, 1738 (2005).
16) S. Y. Chou, P. R. Krauss, and P. J. Renstrom, J. Vac. Sci. Technol. B **14**, 4129 (1996).
17) M. D. Austin and S. Y. Chou, Nano Lett. **3**, 1687 (2003).
18) T. Miteva, A. Meisel, M. Grell, H. G. Nothofer, D. Lupo, A. Yasuda, W. Knoll, L. Kloppenburg, U. H. F. Bunz, U. Scherf, and D. Neher, Synth. Met. **111–112**, 173 (2000).
19) T. Miteva, A. Meisel, W. Knoll, H. G. Nothofer, U. Scherf, D. C. Müller, K. Meerholz, A. Yasuda, and D. Neher, Adv. Mater. **13**, 565 (2001).
20) Z. Zheng, K.-H. Yim, M. S. M. Saifullah, M. E. Welland, R. H. Friend, J.-S. Kim, and W. T. S. Huck, Nano Lett. **7**, 987 (2007).
21) B. Park, Y. H. Huh, and H. G. Jeon, Opt. Express **18**, 19824 (2010).
22) G. Lüssem, F. Geffarth, A. Greiner, W. Heitz, M. Hopmeier, M. Oberski, C. Unterlechner, and J. H. Wendorff, Liq. Cryst. **21**, 903 (1996).
23) M. Barmentlo, N. A. J. M. van Aerle, R. W. J. Hollering, and J. P. M. Damen, J. Appl. Phys. **71**, 4799 (1992).
24) A. Rapini and M. Papoular, J. Phys. Colloq. **30**, C4 (1969).
25) Y. Sato, K. Sato, and T. Uchida, Jpn. J. Appl. Phys. **31**, L579 (1992).
26) H. Yokoyama and H. A. van Sprang, J. Appl. Phys. **57**, 4520 (1985).
27) B. R. Acharya, J.-H. Kim, and S. Kumar, Phys. Rev. E **60**, 6841 (1999).
28) M. B. Feller, W. Chen, and Y. R. Shen, Phys. Rev. A **43**, 6778 (1991).
29) A. Rizzo, C. Nobile, M. Mazzeo, M. D. Giorgi, A. Fiore, L. Carbone, R. Cingolani, L. Manna, and G. Gigli, ACS Nano **3**, 1506 (2009).
30) J. Hu, L. Li, W. Yang, L. Manna, L. Wang, and A. P. Alivisatos, Science **292**, 2060 (2001).